LA-UR--83-1928

DE83 015236

Conf-830425--35

Los Alamos National Laboratory is operated by the University of California for the United States Department of Energy under contract W-7405-ENG-36

TITLE OPTICAL PROPERTIES OF EXPLOSIVE-DRIVEN SHOCK WAVES IN NOBLE GASES

AUTHOR(S) C. R. Jones and W. C. Davis

SUBMITTED TO Los Alamos Conference on Optics, Santa Fe, NM, April 11-15, 1983.

DISCLAIMER

MASTER

Los Alamos Los Alamos National Laboratory
Los Alamos, New Mexico 87545

Optical properties of explosive-driven shock waves in noble gases

C. R. Jones and W. C. Davis

University of California, Los Alamos National Laboratory
P. O. Box 1663, Los Alamos, New Mexico 87545

Abstract

High explosives have been used to shock-heat rare gases to brightness temperatures up to 36 000 K, with large radiating areas. Temperatures were determined from radiometer signals at both 280 and 520 nm. Shock velocities up to 9 mm/μs were used in both plane and cylindrical geometries. Neon, argon, krypton, and xenon gases at atmospheric initial pressure were examined in plane shocks. Using argon, the effects of increased initial pressure were studied. For cylindrical shock expansion in argon, brightness temperatures were measured over a range of shock velocities from 3 to 9 mm/μs. Up to 4% of the explosive energy was emitted as radiation. The shock waves are found to be reasonable approximations to blackbodies.

Introduction

Shock waves in rare gases, driven by high explosive, heat the gas to high temperature. The thermal radiation from the wave is very bright, and the wave can have a large area. Very high power light sources can be made using these shock waves.[1]

High explosive provides compact, cheap, controllable, and safe energy storage, and when detonated, provides high power densities. The explosive used for the studies described here stores about 10 GJ/m^3. The chemical reaction of the explosive takes a few ns, and proceeds at very high pressure, inertially confined by the mass of the explosive itself. The detonation, that is, the transition from unreacted explosive to gaseous products, travels as a wave at about 9 mm/μs. The conversion of chemical energy is thus going on at about 10^{14} W for each square meter of detonation wave area.

In one simple arrangement of an explosive-driven shock tube, or flash charge, the solid explosive forms one wall of the container holding the gas. A plane detonation wave reaches the surface of the explosive, and the gaseous products expand outward, driving the shock-tube gas ahead of them. A shock wave, which is just the boundary between gas that is in motion and gas that has not yet begun to move, propagates out into the gas at a velocity somewhat greater than the interface velocity. In the argon experiments described here, the interface velocity is about 8½ mm/μs and the shock velocity is about 9 mm/μs. The argon gas is compressed into about one-twelfth of its original volume, and the pressure is raised from one atmosphere to about 800 atmospheres. The adiabatic (but not isentropic) compression raises the temperature of the argon to about 25 000 K.

Changing the density of the gas in the shock tube over the easily accessible range, either by changing the temperature and pressure or by using a different gas, doesn't change the velocity of the interface much. The reason for this is that the explosive products, moving at the same velocity on the other side of the interface, are about ten times denser than the compressed shocked gas, and therefore a small decrease in their velocity provides the necessary energy to drive a denser gas. The simple shock wave conservation conditions show that the specific internal energy of the shocked gas is increased in the shock by ½u^2, where u is the velocity of the interface. For our purpose of using shock waves as light sources we require high temperatures, and with the jump in specific internal energy more or less fixed and the same for all gases, we must look for gases with the smallest specific heats. Polyatomic gases have high specific heats because there are many degrees of freedom, and also dissociation, to absorb energy. If the monatomic gases were ideal gases in the interesting temperature and density region, their specific heats would be inversely proportional to their atomic weights. They are not quite ideal, because they are slightly ionized and energy is used for that. For our purpose a monatomic gas with high ionization potential and large atomic weight will have high shock temperature. Xenon is the best choice, and experiment bears out this simple analysis. For most of our work reported here, we used argon because it is so much cheaper.

Explosive-driven shock tubes are very simple devices. There are only two experimental details to be careful about. The obvious one is that the gas must be kept pure, because at temperatures of several tens of thousands of degrees a small amount of an impurity gas can raise the specific heat by a large amount. The second is less obvious. It is imperative to

use precision explosive, and to initiate it smoothly, because the interface where the dense explosive products drive the lighter gas is an unstable interface. Imperfections produced there will grow as the wave moves, product gases will mix with the driven gas, and high temperatures will not be achieved.

The very high temperatures produced in shock waves lead to very high radiated powers, and these cause some effects that may not be anticipated. For example, the xenon shock wave at velocities used here has a temperature of about 36 000 K. A blackbody at this temperature radiates 95 GW/m^2, most of this radiation lying in the vacuum ultraviolet. This much radiation damages windows and mirrors, making some experiments difficult. It also heats the gas at the walls before the shock wave reaches that gas, and the interaction of the wave with the heated gas distorts the shape of the wave. One must be careful to check that the shock wave really has the shape he thinks it has. Some of these effects have been reported by Shreffler and Christian.[2]

Shock Tubes

The shock tubes used to study the ultraviolet and visible emission from planar shock waves are designed to be filled by first evacuating the tube, and then filling to the desired pressure with the chosen gas. This feature was necessary for the expensive rare gases, but argon fillings were made by simply flushing the tube with 10 or more volumes of gas. The tube design is shown schematically in Fig. 1. The explosive driver made up one end of the tube; the seal to it was made with an O-ring. A sample tube was provided so that a gas sample could be taken and analyzed with a mass spectrograph.

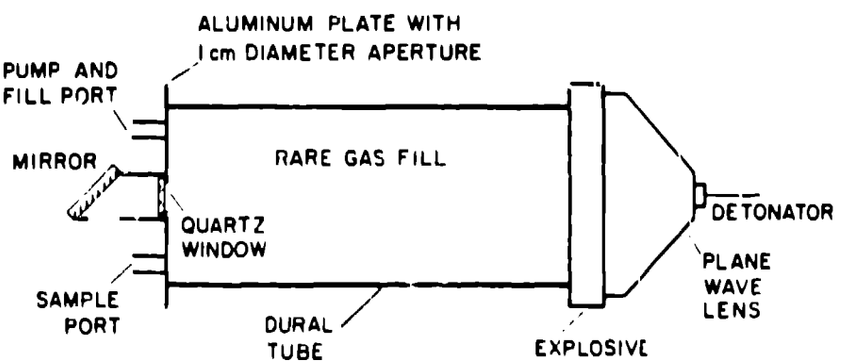

Fig. 1. Schematic of explosive flashlamp or argon flashcharge: typically the tube is 10 cm in diameter by 30 cm in length. Variations include cardboard material for the tube, no window over the aperture, or no planewave lens on the explosive.

The explosive used for these experiments was PBX-9404, a plastic-bonded composition containing 94% HMX and having a density of 1.84 g/cm^3. It is a high-quality material, appearing much like any good plastic, and is a very high-energy explosive. Initiation of the explosive used a planewave lens, which is a device that initiates the explosive over its entire surface simultaneously.

The luminous shock wave fills the cross-section of the tube and moves from the explosive toward the other end. For our purposes of measuring shock brightness a defining aperture is needed, which is provided by a precise hole in the end plate as shown in Fig. 1. When required, a quartz window was glued beyond the aperture. A front-surface aluminum mirror was used to turn the light beam. This turning was necessary to keep the fragments of the metal tube, formed by the explosion, from hitting the measuring apparatus.

Brightness Measurements for Plane Waves

The shock tubes were set up at an explosive firing site, about 6.5 m outside one wall of a heavy concrete and steel bunker. Optical detectors were positioned just inside a quartz window, which was firmly secured in the wall. The shock tube was carefully aligned so light from the center of the shock wave went through the aperture to the detectors. The detectors, ITT F-4018 biplanar photodiodes with S-5 response, were calibrated absolutely against standard lamps. The recommended bias voltage of 1 kV was applied. A bandpass filter centered at 280 nm with a passband of 20 nm FWHM and peak transmittance 17% was mounted on one

detector. A filter with passband centered at 520 nm with 9 nm FWHM and 60% peak transmittance was mounted on another. The coaxial signal cable from each detector went to oscilloscopes and was terminated with 50 ohms.

Some typical oscilloscope records are shown in Fig. 2. The rise time of the light signal is not seen in these records except when neon is used, for which it takes an appreciable time to achieve an optically thick layer of gas. After the initial peak the intensity decreases; this decrease is caused in part by the pressure distribution in the explosive

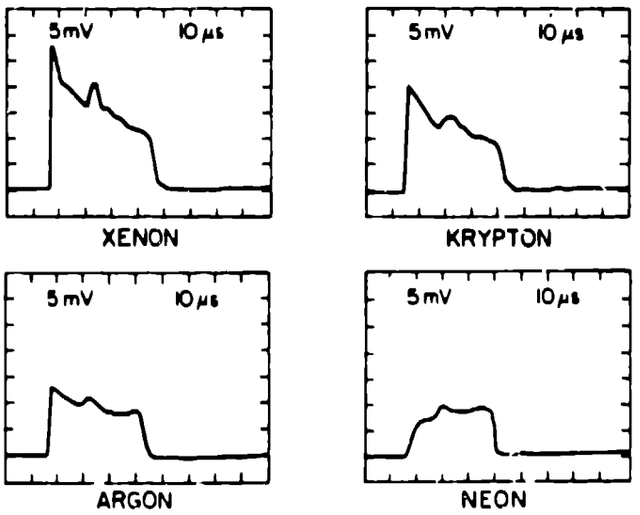

Fig. 2. Ultraviolet signals from flash charges containing xenon, krypton, argon, and neon. Wavelength: 280 nm. Spectral radiance calibration: L_λ = 400 W/cm²-nm-sr per division.

detonation wave, where the pressure falls behind the front, and in part by radiation damage to window, mirror, and air in the light path. The shock velocity is not constant, but decreases as the shock wave runs down the tube. In argon, for example, the shock velocity changes with time according to

$$v = 9.00 \exp(-0.013t) \text{ mm}/\mu\text{s} ,$$

with t in μs. At about 13 μs after the light appears, in each gas, a bump appears in the oscilloscope trace. This signal change arises because the radiation from the gas heats the tube wall and the gas near the wall. The shock wave runs faster in the hot gas, and its shape is perturbed. A wave from the wall converges to the center at 13 μs, producing the bump. After that time, more reflections occur. The pertinent data from these records is the peak brightness, the value just after the light appears, when the shock front is plane and the shock velocity is 9.1 mm/μs. Table 1 gives a summary of the data. Only with argon was radiometric data obtained at 520 nm.

Table 1. Shock Wave Temperatures

Gas	Initial Pressure	T, λ = 280 nm	T, λ = 520 nm
Neon	590 torr	22 000 K	
Argon	590	27 000	23 000
Argon	3540	26 000	23 000
Krypton	590	30 000	
Xenon	590	36 000	

Conical and Cylindrical Shock Waves

Conical and cylindrical shock waves were generated using long right-circular cylinders of explosive. The explosive used was PBX-9501, with density 1.84 g/cm^3, a material very similar to the PBX-9404 used for the plane wave studies. The cylinders were 51 mm in diameter.

Two experiments were done with the cylinder of explosive initiated at a point on one end, forming a steady detonation propagating along the cylinder at a constant velocity of 8.75 mm/μs. The cylinder was surrounded with argon gas contained in a large box. One wall of the box was glass, and Fig. 3 is a photograph of the shock wave in argon taken through that window. The shock velocity can be obtained from the angle the wave makes with the cylinder, measured from the photograph. An image-intensifier camera with a shutter time of about 20 ns was used to take the photograph.

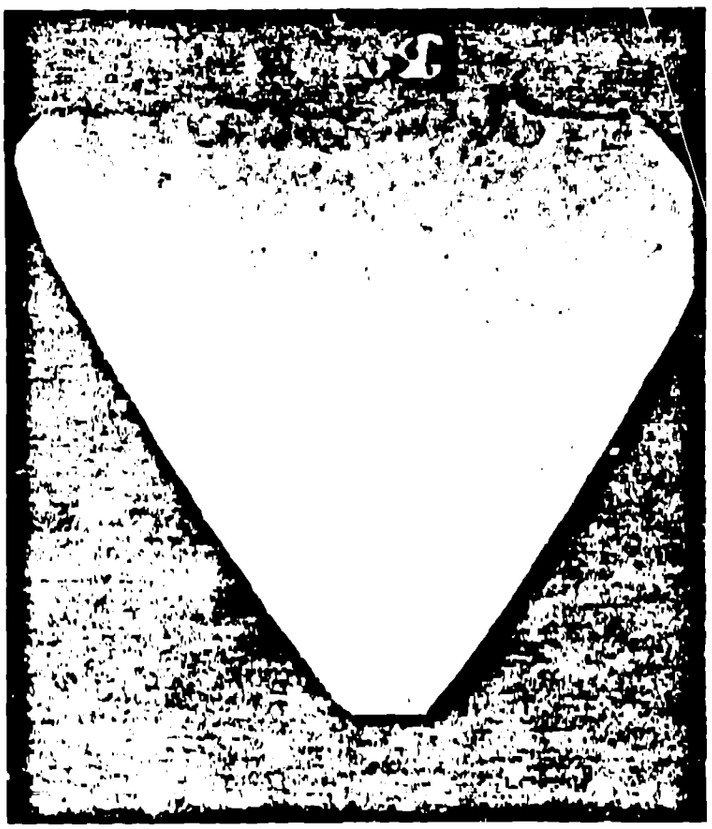

Fig. 3. Side view of light from the shockwave in argon driven by a cylinder of explosive initiated at one end. The perturbations caused by the joints in the charge are visible, but it can be seen at the edges that they cause almost no variation in the shock shape. The regular cross hatching is caused by the structure of the fiber-optics output plate of the camera tube. The flat base is 5 cm across. Shot No. C-5083-D. Test UV-16.

One experiment was done with the explosive cylinder initiated simultaneously along its axis using a pair of line-wave generators. A diagram of the system, with an enlarged view of a line-wave generator is shown in Fig. 4. A photograph of the cylindrically expanding shock wave is shown in Fig. 5. The shock position and wave velocity were obtained from similar photographs multiply exposed at accurately known times.

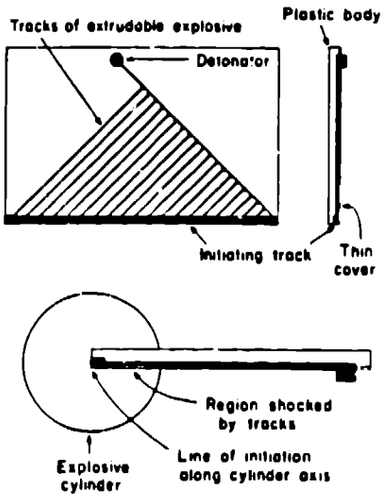

Fig. 4. Diagram of a line-wave generator, and end view of the axially initiated explosive charge. The line-wave generator is initiated at one point, and the detonation wave in the tracks of extrudable explosive runs the same distance in every track. The explosive is contained in the thick plastic form, and has only a thin cover over it.

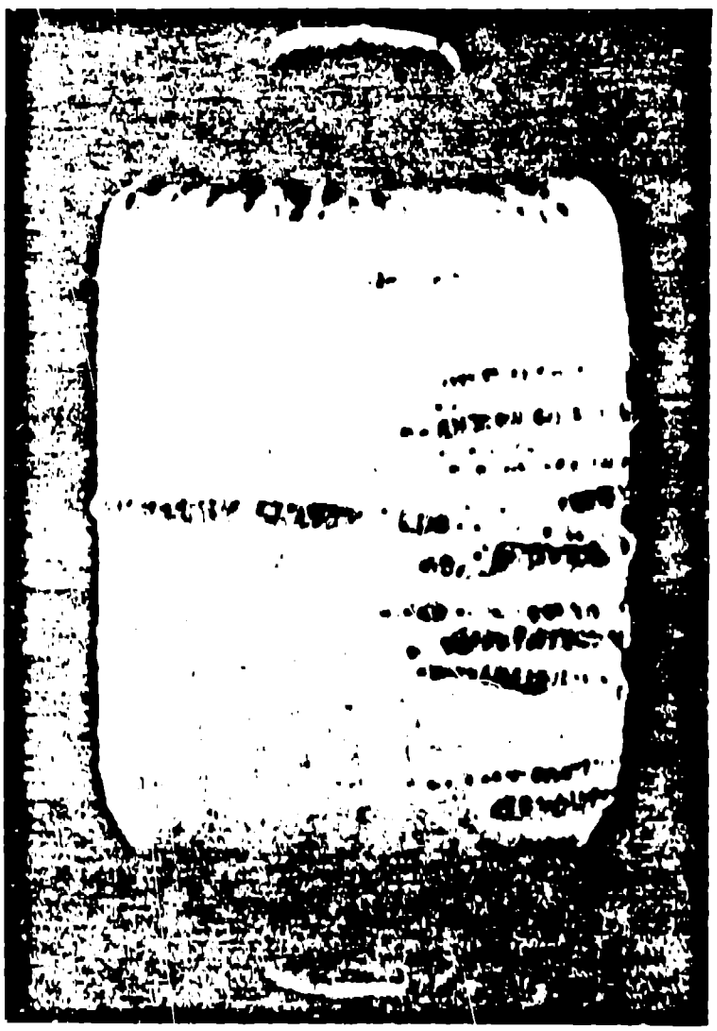

Fig. 5. Photograph of a cylindrically expanding shockwave. The perturbation on the left is caused by the interaction between the two line-wave generators. The extra ones on the right are caused by the shock transmitted through the thin plastic cover of the line-wave generator by the extrudable explosive. Shot No. C-5101-B. Test UV-23.

Brightness Measurements for Conical and Cylindrical Waves

While one wall of the box containing the argon was glass to allow photography of the shock waves, another wall was opaque with apertures for brightness measurements. The measurement apparatus was the same as for the planar shock measurements, except that two bunker windows were used, and there were two apertures in the box. One aperture was on-axis, and the other was 180 mm off-axis at the same level. The light from one aperture went to detector(s) in one window, and light from the other aperture to the other window and its detector(s). Table 2 lists results of these measurements for the conical shock. The shock wave is seen to deviate somewhat from the ideal behavior of a Lambertian radiator, in that the oblique temperatures are consistently less than the on-axis ones.

Table 2. Radial-Shock Temperatures at Various Times

Test	View	Time*, μs	Temperature, K
UV-15	Normal	48	18,500 ± 500
		74	16,600 ± 1300
		98	15,000 ± 1700
	Oblique	74	14,700 ± 200
		98	12,100 ± 200
UV-16	Normal	48	18,500 ± 500
		70	16,800 ± 1200
		94	14,200 ± 1300
	Oblique	70	14,300 ± 200
		94	10,800 ± 200

*Time elapsed between trigger pulse to detonator and reading of radiometer signal.

The velocity of the wave decreases as the shock expands. Fig. 6 is a plot of shock wave velocity vs time for the conical and cylindrical experiments. The variation of brightness with time can be converted into a plot of brightness temperature vs shock velocity, as shown in Fig. 7 for the cylindrical shock. The graph seems to show that the brightness

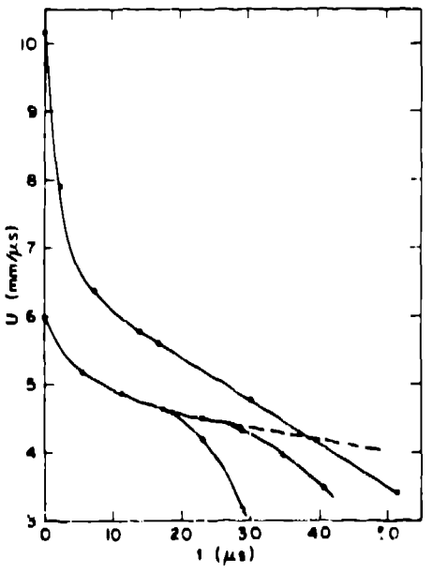

Fig. 6. Plot of shock velocity vs time for the second and third experiments. The lower curve is for the end-initiated second experiment. The points depart from a smooth curve where the flow has not yet become steady. There are two parts to it because there were photographs taken at two times. The upper curve is for the axially initiated third experiment. The outward-directed detonation wave gives a high initial shock velocity.

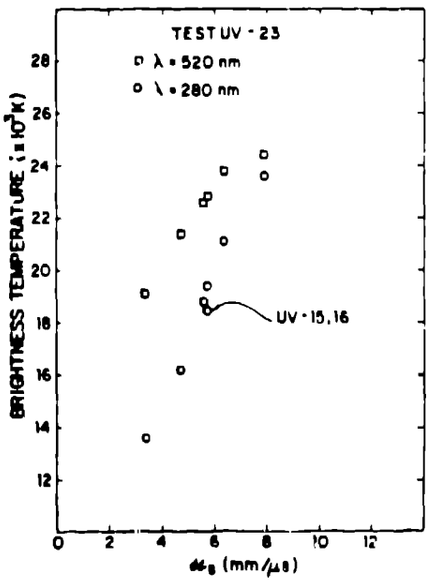

Fig. 7. Dependence of the brightness temperature on the shock velocity for a cylindrically expanding shockwave in argon gas. With the exception of the point marked otherwise, the data are from different times of expansion in Test UV-23.

temperature in the ultraviolet is more strongly dependent on shock velocity than, and everywhere less than, the brightness temperature in the visible, but we believe that to be false. Spectrographic experiments made on planar shock waves of similar strength show strong absorption by magnesium from the defining aperture at 277.983, 278.142, 279.553, 280.267, and 285.213 nm, and silicon at 288.195, near the center of the filter passband. The intense radiation from the shock wave heats the dural aperture plate enough to vaporize the metal, and the resulting vapor may absorb a substantial fraction of 280 nm emission. In retrospect, it seems that dural was a bad choice for the aperture plates.

There is no absorption from the metal vapor in the passband of our visible filter, but the spectrum shows absorption by argon at 516.228 and 518.775 nm in the shock wave itself. It is possible that this absorption is responsible for some of the temperature difference that appears for different wavelengths in Table 1.

The radius of the cylindrical shock wave, found by analyzing the series of photographs of it at different times, is given by

$$r = 8.322\ [1 - \exp(-t/2.77)] + 6.679t - 0.0318t^2 \quad .$$

The temperature as a function of time (for 520 nm, where there is no metal vapor absorption) is given in Fig. 7. The area of the shock wave is known from the expression above, and, if the shock radiates as a blackbody, the total energy radiated can be calculated. The values are tabulated in Table 3. The explosive energy was 5×10^6 J. The radiation during the first 50 μs is about 4% of the explosive energy. If xenon had been used instead of argon the yield might have been as much as 16%.

Table 3. Radiometric Properties of Cylindrical Shock Surface

t, μs	r, cm	A, cm^2 $2\pi r\ell$	T, kK [a]	$M = \sigma T_2^4$ [b] W-cm	$A\sigma T^4$ W
0+	2.54	479	26.2	2.67×10^6	1.28×10^9
7.23	8.05	1517	24.8	2.15×10^6	3.25×10^9
14.20	12.2	2300	22.8	1.53×10^6	3.52×10^9
30.23	20.7	3902	21.4	1.19×10^6	4.64×10^9
51.15	29.2	5506	19.1	7.55×10^5	4.16×10^9

[a] Temperature measured at λ = 520 nm.

[b] Total radiated power per square centimeter (emittance) of shock surface.

Discussion and Comparison with Other Results

Optical radiation from shock fronts has been investigated both experimentally and theoretically for several decades. Zel'dovich and Raizer in their textbook[3] discuss this subject in some detail, with particular emphasis on shock waves in air. Of interest here is that for shock waves of the strength used in our studies the front radiates as a blackbody. They also treat in detail the phenomenon of the preheating layer. This layer lies in front of the radiating shock front and attenuates the light on its path to the detection system. Hard ultraviolet radiation, from sufficiently hot shock fronts, induces opacity in the otherwise cold gas through photoionization, photoexcitation, and photochemistry in this layer. Screening of the shock front from the detectors therefore occurs, whose magnitude increases strongly with shock velocity and which depends also upon the gas and wavelength being observed. For example, in air strong screening occurs for shock temperatures in excess of 90 000 K,[3] beyond which the optically measured brightness temperature is substantially less than the true temperature behind the front.

It is well known that the absorption of oxygen begins at 186 nm and extends downward into the harder ultraviolet. For the brightness temperatures of ~25 kK measured in our experiments, the emission peak of the corresponding blackbody radiation occurs at a λ = 116 nm. At this wavelength the absorption coefficient of air[3] is ~120 cm^{-1}. For experiments conducted here without a window over the source aperture, light-induced phenomena in the air path are expected. This is a likely source of absorption, although none was observed in our spectra of argon flashchamber.

Zatsepin et al.[4] have measured the luminescence of shock fronts in air, argon, and xenon over a large range of shock velocities. Brightness of the fronts was observed at 300, 430, and 560 nm and at angles of incidence to the shock front of 90° and 45°. One important results from this work was that at higher velocities the normal-incidence radiation usually indicated a significantly higher temperature than the 45° radiation. In this respect, our results of Table II are consistent with theirs. They ascribe this behavior to the greater pathlength through the absorbing preheating layer for the oblique path. According to their results at lower velocities, however, the opacity of the preheating layer should be insufficient to affect this difference at our velocities. They do point out that for longer light pulses the screening layer can be more absorbing. The duration of our light pulses appears to be much longer than theirs, so a screening layer could have been responsible for the temperature differences in Table II.

Available data for shock waves in argon are plotted in Fig. 8. The ultraviolet points from Ref. 4 are shown along with Soviet theoretical predictions. Also included are data points from this work and theoretical curves of Kerley.[5] A single data point from each of the works of Zinn et al.,[1] Model',[6] and Kiselev and Krokhin[7] is also plotted. The experimental points from Zatsepin et al. are in excellent agreement with Soviet equation-of-state theory up to shock velocites of 14 km/s, where subsequent departure from theory is attributed to the screening layer. Our ultraviolet data are in very good agreement with Soviet theory. Our 520-nm data show substantial departure from the Soviet curve in Fig. 8. We do not know why our 520-nm points are above the curve for the cylindrical tests and below it for the average of planar shocks. For both visible and uv, our data indicate a fall-off from the trend for the higher velocities. Zatsepin et al. do not observe this fall-off until velocities of 15 km/s are reached. The data point from Model' in Fig. 8 represents a large departure from theory.

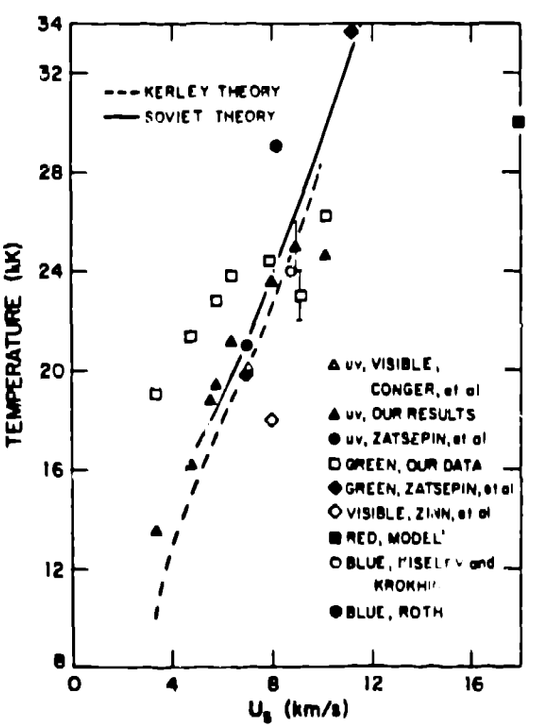

Fig. 8. Measured and theoretical brightness temperatures of shock fronts in argon gas as a function of shock velocity. Our points are from cylindrical expansions (UV-23), except for those points with error bars that represent averages of planar shock results.

In Fig. 9 available brightness temperature data for xenon are shown along with theoretical curves. Most of the points are from Zatsepin et al. recorded at λ = 430 nm. One point each from our work and from Model' is included. It is thought that the screening layer is responsible for most of the points lying below the curve.[4] Again, however, our results agree rather well with those from Ref. 4. Kerley's theory,[5] covering 2-6 km/s, is in excellent agreement with the Soviet theoretical results. He also computed temperatures for argon at ρ_0 = 0.006 g/cc density (~4.6 local atmospheres), obtaining ~10% higher temperatures near 9 mm/μs shock velocities than at 1 atm. This result agrees with our data.

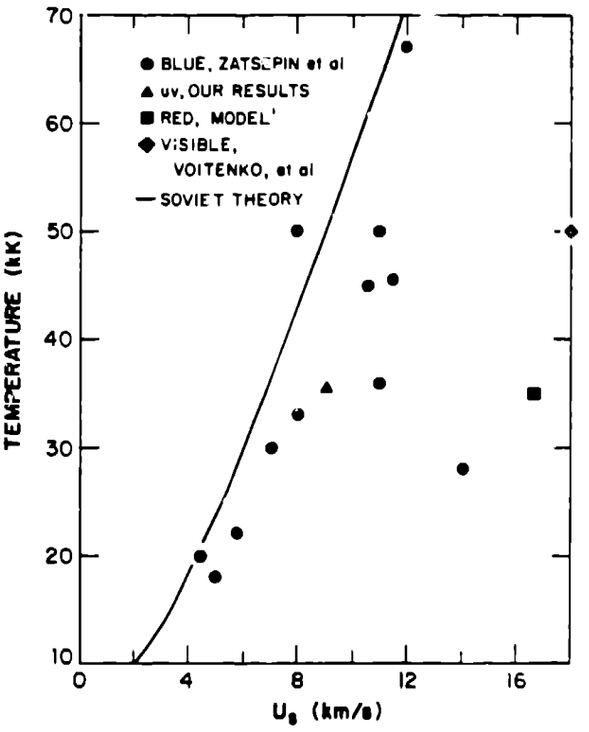

Fig. 9. Measured and theoretical brightness temperatures of shock front in xenon gas as a function of shock velocity. Our datum is from planar shock wave studies.

Other rare gases have been investigated, but less extensively. Model' reports[6] a temperature of 34 kK for a 17.2-km/s shock wave in krypton. Roth[8] measured 38 kK for a velocity of 8.3 km/s, somewhat higher than our value of 30 kK. Tsikulin and Popov[9] report a temperature of 32 kK at λ = 280 nm and at a velocity of 8-9 km/s. Our value, obtained at that wavelength and similar shock velocity, is in good agreement with this result.

For neon, also, the measurements of Tsikulin and Popov[9] are in very good agreement with our results, shown in Table 1.

Summary and Conclusions

High explosives have been used to shock-heat rare gases to measured brightness temperatures up to 36 000 K. The area of the radiating shock fronts was large in both the planar and cylindrical geometries used. Close agreement between temperatures measured at both ultraviolet and visible wavelengths indicates that the sources are blackbody radiators. The continuous nature of the emission spectrum of the shockfront supports this conclusion.

The planar shocks reported here had radiating areas of 75 cm^2. Shock waves through argon gas were studied extensively. At one local atmosphere the temperature measured for the emission of an argon shock at its peak velocity of 9 mm/μs was 25 kK. At six times this pressure, the measured temperature was approximately 10% higher.

Substitution of other rare gases into the shock tube resulted in some measured emission signals that are proportional to the square root of the atomic weights. For Xe a peak temperature of 36 kK was measured.

In radially expanding shock waves, stable large-area fronts in argon were observed. The temperatures and profiles of shock fronts were measured using two initiation schemes. Temperature and velocity as a function of time were determined and compared with results of other research.

For the axially initiated explosive, a cylindrical shock wave having an area beginning at 480 cm^2 and expanding to 5500 cm^2 was studied. During this expansion, the temperature fell from 26 kK to 19 kK, but the area-integrated radiation from the front continued to rise over the full 50-μs observation time. The total optical energy according to a blackbody calculation was 2×10^5 J for an explosive energy to optical energy yield of 4%. Greater efficiencies using xenon can be expected.

More information can be found in a report[10] that describes all our measurements in detail.

References

1. J. Zinn, W. C. Davis, T. R. Schwartz, R. C. Anderson, and W. D. Gould, "Theoretical and Experimental Studies of Strong Shock Waves in Air," Proceedings of the DNA Atmospheric Effects Symposium, San Diego, April 1973.
2. R. G. Shreffler and R. H. Christian, "Boundary Disturbances in High-Explosive Shock Tubes," J. Appl. Phys. 25, 324-331 (1954).
3. Ya. B. Zel'dovich and Yu. P. Raizer, Physics of Shockwaves and High-Temperature Hydrodynamic Phenomena (Academic Press, New York, 1966).
4. Y. A. Zatseptin, E. G. Popov, and M. A. Tsikulin, "Luminance of Shock Wave Fronts in Certain Gases," Sov. Phys. JETP 27, 63-66 (1968).
5. G. Kerley, X-7, Unpublished Los Alamos Results (1982). He used ionization equilibrium theory described in LA-8062.
6. I. Sh. Model', "Measurement of High Temperatures in Strong Shock Waves in Gases," Sov. Phys. JETP 5, 589-601 (1957).
7. Yu. N. Kuselev and V. Z. Krokhin, "Measurement of Radiation from Strong Shock Waves in Gases Using Low-Inertia Pyroelectric Detectors," Translated from Fiz. Goreniya i Vzryva 12 956-959 (1976).
8. J. Roth, "Measured Temperatures of Strong Shock Waves in Argon," J. Appl. Phys. 35, 1429-1433 (1964).
9. M. A. Tsikulin and Ye. G. Popov, Radiating Properties of Shock Waves in Gases (Nauka, Novosibirsk, 1977).
10. C. R. Jones and W. C. Davis, "Optical Properties of Explosive Driven Shock Waves in Noble Gases," Los Alamos Report LA-9475-MS, Sept. 1982.